

11

# Electronic Structural and Bulk Properties of ScSe: *ab initio* Study

© P. Bhardwaj, S. Singh

High Pressure Research Lab., Department of Physics, Barkatullah University, Bhopal, India

E-mail: purveebhardwaj@gmail.com

(Received November 25, 2015

In final form, April 19, 2016)

Electronic, structural and bulk properties of scandium selenide, ScSe have been reported in the present paper. These properties have been studied using first principle calculations as well as the interionic potential model modified with covalency effect. The Gibbs free energy and enthalpy calculations show that present compound undergoes a structural phase transition from the NaCl-type structure to the CsCl-type structure. The stability of the present compound is discussed in terms of electronic band structure and density of states. The calculated equilibrium structural parameters are in a good agreement with the available experimental results.

Authors are thankful to Department of Science & Technology (DST), New Delhi for the financial support to this work. One of the authors (PB) is grateful to Department of Science & Technology (DST), New Delhi for awarding WOS-'A' (Grant no. SR/WOS-A/PS-17/2013).

## 1. Introduction

The rare earth chalcogenides and pnictides have attracted more attention due to their electronic structures and magnetic properties which are sensitive to temperature, pressure and impurity effects. These compounds are complicated to be fabricated into single-phase crystals. Their electronic structure and the experimental picture are also difficult to understand. Frequent attempts have been made to understand the electronic properties of rare earth chalcogenides and pnictides in the past [1–5]. They have various practical applications in the field of non-linear optics, electro-optic components, glass-making, grinding alloys, composites lasers, phosphors lasers, and electronics [5–8].

Among these compounds the rare earth chalcogenides are perspective materials. During the high-pressure resistivity studies they undergo a pressure induced electronic phase transition [9]. For some rare earth chalcogenides this transition is found to be continuous while discontinuous for others. This class of compounds is characterized by metals, semiconductors and insulators. These compounds have high melting point, good thermal stability, interesting magnetic and thermal properties [10]. High pressure X-ray diffraction study shows an anomalous decrease in volume with pressure, which is attributed to the 4f-5d electronic transition in rare earth chalcogenides [11]. Chatterjee et al. [12] have investigated the compressibility of the rare earth monochalcogenides up to 300 kbar using high-pressure x-ray-diffraction techniques. The high-pressure structural (B1–B2) phase transition and the elastic properties of ScSe using the full-potential augmented plane wave plus local orbitals method (FP-APW + LO) with the generalized-gradient approximation (GGA) exchange-correlation functional have been reported by Maachou et al. [13]. At ambient conditions, the chalcogenides of scandium crystallizes in the six-fold coordinated NaCl-type (B1) structure with space

group symmetry  $Fm\bar{3}m(225)$ . They are expected to undergo pressure-induced first order phase transition to eight-fold coordinated the CsCl-type (B2) structure with space group symmetry  $Pm\bar{3}m(221)$ , as is observed in many other heavier RE chalcogenides. In the above discussed papers [9–13], the B1–B2 structural phase transition and elastic properties for these compounds have been reported. However, there is no sufficient data on rare earth chalcogenides. ScSe among these rare earth chalcogenides has very less work to its credit.

So we have worked in this line to add some more study on ScSe by exploring its electronic, structural and bulk properties. These properties are investigated using two approaches: the model calculation (Approach I) and the first principle calculations (Approach II). The ground state properties for B1-type ScSe are studied by the first principle tight binding linear muffin tin orbital (TB-LMTO) method. The comparative study of a structural phase transition and volume collapse of the present compound has been represented from both approaches. In addition, we report on the electronic band structure (BS) and density of states (DOS) for ScSe. The organization of the present paper is as follows: The method of computation of both approaches is described in Section 2. The Modified interaction potential model (MIPM) with including covalency effect is described in Section 2.2. The results are discussed in Section 3. In subsections 3.1 and 3.2, the structural and electronic properties of ScSe at ambient and high pressure are reported respectively. Finally, in Section 4, we have given conclusion of the present results.

## 2. Methods of Calculation

2.1. First principle calculations. Scandium selenide ScSe considered in the present work crystallizes in the NaCl-type ( $Fm\bar{3}m, 225$ ) structure at ambient conditions.

The scandium atom is positioned at (0,0,0) and selenium at (1/2,1/2,1/2). Under pressure they transform into the CsCl-type ( $Pm\bar{3}m$ , 221) structure in which Sc and Se atoms are positioned of (000) and (1/2, 1/2, 1/2) respectively. For loosely packed structures, empty spheres are introduced in the appropriate concentrations in the NaCl phase without breaking the crystal symmetry. Since the TB-LMTO method works well for the closed packed structures, while the present compound belongs to the NaCl phase at ambient conditions, which is not a close packed one. Therefore, for these loosely packed structures the two equivalent empty spheres at position (0.25, 0.25, 0.25) and (0.75, 0.75, 0.75) have been introduced in such a way that they do not break the crystal symmetry [14]. For the CsCl structure, these empty spheres are not needed because it is a closed packed structure. The electronic band structures are calculated using the self-consistent tight binding linear muffin-tin-orbital (TB-LMTO) method [15,16] within the local density approximation (LDA) [17]. As regards the long-range/short-range decomposition of the exchange functional, the results of this work suggest that the LDA is more accurate for the short-range contribution rather than for the long-range contribution [18]. The van Barth and Hedin [19] parameterization scheme has been used for the exchange correlation potential. To minimize errors in the LMTO method, the combined correction terms are included. These terms account for a non spherical shape of the atomic spheres and the truncation of the higher partial waves inside the sphere. Between the atoms, charge flows according to the electronegativity criteria [20]. The partial waves of  $s$ ,  $p$ ,  $d$  and  $f$  states are taken into account. The  $E$  and  $k$  convergences are checked subsequently to achieve better accuracy. The calculations were performed for 512 k points (grid of  $8 \times 8 \times 8$ ) in the Brillouin zone for both  $B1$  and  $B2$  phases. To obtain the total energy and partial density of states, the tetrahedron method [21] of Brillouin zone integration is used. The total energy was computed by reducing the volume from  $1.05V_0$  to  $0.60V_0$ , where  $V_0$  is the equilibrium cell volume. The calculated total energy was fitted to the Birch equation of states [22] to obtain the pressure volume relation. The pressure is obtained by taking the volume derivative of total energy. The bulk modulus  $B = -V_0 dP/dV$  is also calculated from the  $P-V$  relation. The stability of a particular structure is decided by the minima of the enthalpy. The phase transition pressure can be obtained by matching enthalpies of both structures such that the difference of enthalpy  $\Delta H (= H_{B2} - H_{B1})$  becomes zero at transition pressure.

**2.2. Model calculation.** The natural consequence of application of pressure on the crystals is the compression, which in turn leads to an increased charge transfer (or three-body interaction effects)[23] due to the existence of the deformed (or exchanged) charge between the overlapping electron shells of the adjacent ions.

These effects have been incorporated in the Gibbs free energy ( $G = U + PV - TS$ ) as a function of pressure and three body interactions (TBI), which are the most dominant

**Table 1.** Input and output parameters of ScSe

Crystal	Input parameters		Output parameters		
	$r, \text{\AA}$	$B, \text{GPa}$	$b$	$\rho$	$f_m(r)$
ScSe	2.699 <sup>a</sup>	95.92 <sup>b</sup>	10.6387	0.247	0.00232

$a - [25], b - [13]$

among the many body interactions. Here,  $U$  is the internal energy of the system equivalent to the lattice energy at temperature near zero and  $S$  is the entropy. At temperature  $T = 0$  K and pressure ( $P$ ), the Gibbs free energies for  $BX$  ( $X = 1, 2$ ) phase are give by

$$G_{BX}(r) = \frac{-\alpha_m^X Z^2 e^2}{r^X} - \frac{12\alpha_m^X Z e^2 f_m(r)}{r^X} - \left[ \frac{C^X}{r^{X^6}} + \frac{D^X}{r^{X^8}} \right] + 6b\beta_{ij} \exp[(r_i + r_j - r^X)/\rho] + 6b\beta_{ii} \exp[(2r_i - Y_X r^X)/\rho] + 6b\beta_{jj} \exp[(2r_j - Y_X r^X)/\rho] + PV_{BX}(r^X), \quad (1)$$

where  $X = 1$  (Phase 1 =  $B1$ ),  $2$  (Phase 2 =  $B2$ ), and  $Y_x = 1.414, 1.154$ , for NaCl ( $B1$ ) and CsCl ( $B2$ ) structures respectively. Here,  $\alpha_m^X$  is the Madelung constant,  $C$  and  $D$  are the overall van der Waals coefficients for the NaCl and CsCl structures, respectively,  $\beta_{ij}$  ( $i, j = 1, 2$ ) are the Pauling coefficients defined as  $\beta_{ij} = 1 + (Z_i/n_i) + (Z_j/n_j)$  with  $Z_i$  ( $Z_j$ ) and  $n_i$  ( $n_j$ ) as the valence and the number of electrons of the  $i$  ( $j$ )<sup>th</sup> ion;  $Ze$  is the ionic charge and  $b$  ( $\rho$ ) are the hardness (range) parameters,  $r$  is the nearest neighbour separations  $f_m(r)$  is the modified three body force parameter which includes the covalency effect with three body interaction,  $r_i$  ( $r_j$ ) are the ionic radii of ions  $i$  ( $j$ ).

These lattice energies consist of the long range Coulomb energy (first term), three body interactions corresponding to the nearest neighbour separation  $r$  (second term), vdW (van der Waals) interaction (third term), energy due to the overlap repulsion represented by Hafemeister and Flygare (HF) type potential and extended up to the second neighbour ions (fourth, fifth and sixth terms).

Covalency effects have been included in three-body interactions in the second terms of lattice energies given by Eq. (1). The modified three body parameter  $f_m(r)$  becomes

$$f_m(r) = f_{TBI}(r) + f_{cov}(r). \quad (2)$$

The relevant expressions of  $f_{TBI}(r)$  and  $f_{cov}(r)$  are given in our earlier works [23,24]. The Gibbs free energies contain three model parameters [ $b, \rho, f_m(r)$ ]. The values of these parameters have been evaluated according to the method used earlier [25,26]. Using these model parameters and the minimization technique, phase transition pressures of the present compound have been computed. The input data [13,27] of the crystal and calculated model parameters are listed in Table 1.

**Table 2.** Phase transition and volume collapse of ScSe

Crystal	Phase transition pressure, GPa		Volume collapse, %	
	Present	Others	Present	Others
ScSe (Approach I)	52.0	53.65 <sup>a</sup>	5.0	5.24 <sup>a</sup>
(Approach II)	53.0	–	5.15	–

<sup>a</sup> – [13]

### 3. Results and discussion

**3.1. Structural properties.** The structural stability of ScSe is determined by calculating the Gibbs free energies of real and hypothetical phases followed by the technique of minimization. The phase transition occurs when the difference of the Gibbs free energy ( $\Delta G$ ) approaches zero ( $\Delta G \rightarrow 0$ ). At the transition pressure ( $P_t$ ), the present compound undergoes a (B1–B2) transition associated with a sudden collapse in volume showing a first order phase transition. The B1–B2 structural phase transition pressure for ScSe at 52.0 GPa is shown in Fig. 1, which is computed from Approach I. The present phase transition pressure has been shown by arrow in Fig. 1 and has been reported in Table 2 along with the comparisons with the available results [13]. To determine the structural stability of ScSe the total energies in the NaCl-type structure have been calculated from Approach II. The calculation of the phase transition pressure is carried out by estimating enthalpy in both structures as described earlier in Section 2. The total energies are plotted against different compressions for the present compound in Fig. 2. The minimum of all curves define the equilibrium volume  $V_0$  (or equilibrium  $a_0$ ), which is found to be  $49.68 \text{ \AA}^3$  for ScSe, and the corresponding parameter is  $5.389 \text{ \AA}$ , which is underestimated by 5.15%. Our results are compared with those of [13]. It is clearly seen from Fig. 2 that the trend is same as reported by others [13].

Further, we have computed the relative volume changes  $V(P)/V(0)$  corresponding to the values of  $r$  and  $r'$  at different pressures and plotted them against the pressure in Fig. 3 for ScSe. The values of the volume collapses (%) are given in Table 2 from both the approaches. It is clear from Table 2 and Fig. 3 that our calculated volume collapses —  $\Delta V_{(p)}/V_0$  from Approach I (Approach II) are 5.0% (5.15%) for the present compound. Our results on volume collapses for the present compound are close to values obtained in [13].

**3.2. Elastic properties.** The elastic constants of a solid are related to different fundamental properties. Interatomic bonding, equation of state and phonon spectra can be studied based on the knowledge of these constants. They are thermodynamically linked with specific heat, thermal expansion, Debye temperature and Gruneisen parameter. The calculations of the bulk elastic properties play a crucial role in the solid state physics. The bulk

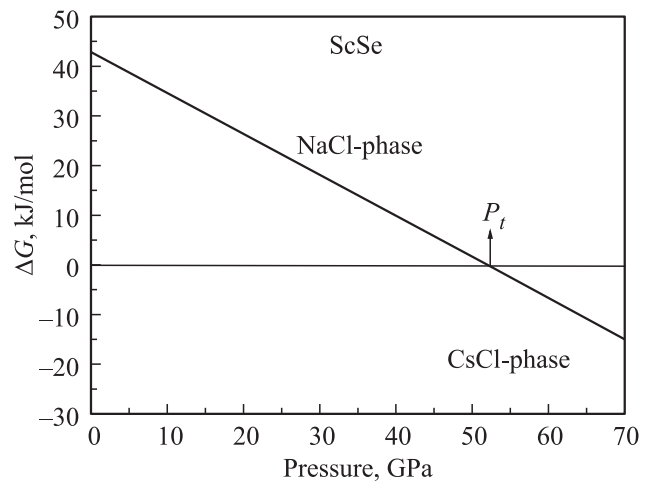


**Figure 1.** Variation of Gibbs free energy change  $\Delta G$  with pressure for ScSe.

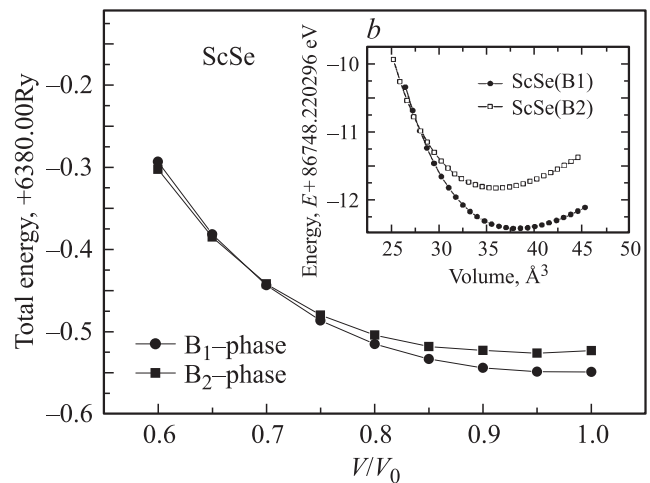


**Figure 2.** Variation of total energy with relative volume for the NaCl and CsCl phases for ScSe.

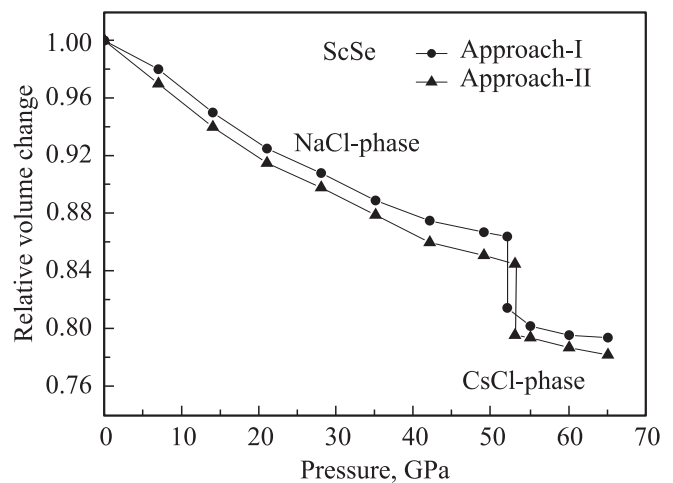


**Figure 3.** Volume change versus pressure. Solid circle and solid triangles represent present Approach I and Approach II respectively for ScSe.

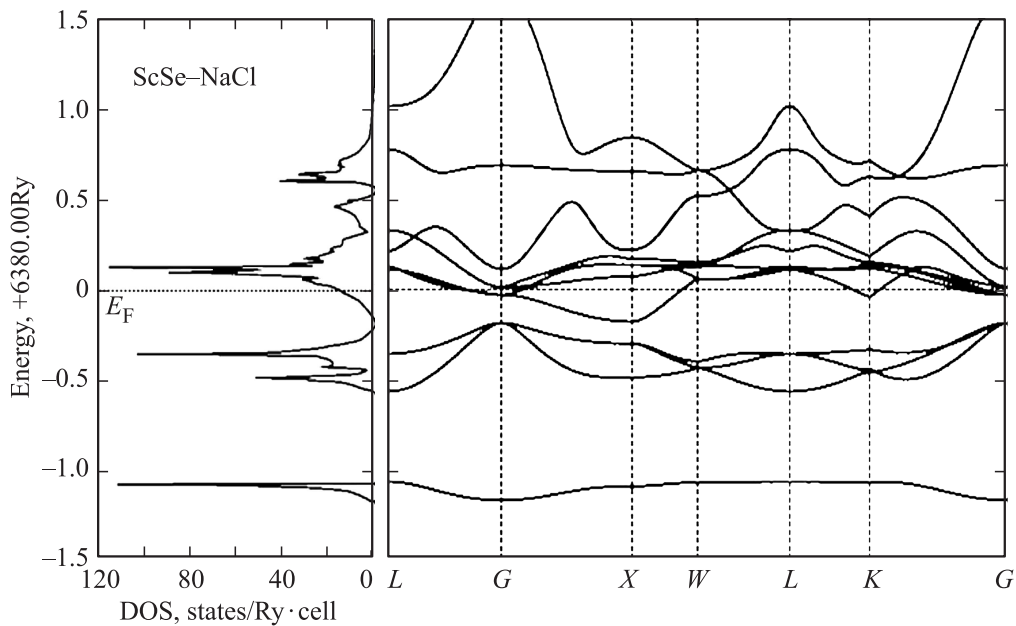


**Figure 4.** Electronic Band structure (BS) and total density of states of ScSe in the NaCl phase.

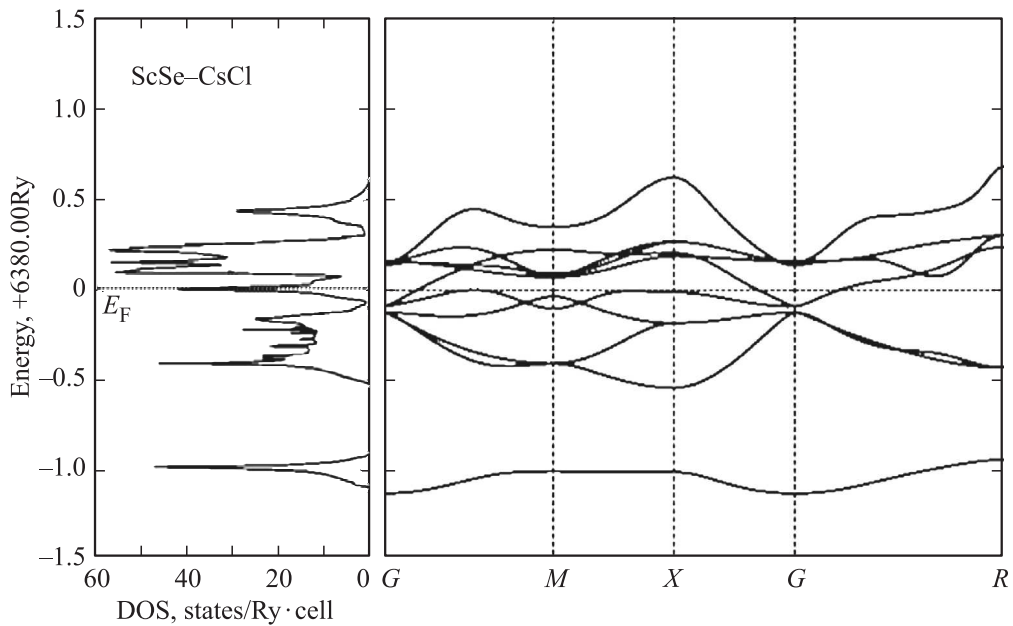


**Figure 5.** Electronic Band structure (BS) and total density of states of ScSe in the CsCl phase.

properties are of importance in geological formations and for industrial applications. The hardness of a material can be determined more accurately by using the bulk modulus. The expression for the bulk modulus is given by  $B = (C_{11} + 2C_{12})/3$ . The computed values of the bulk modulus and pressure derivative of the bulk modulus ( $B'$ ) are given in Table 3. The calculated values of the bulk modulus of ScSe from first principle calculation are also presented in Table 3. Our calculated value of bulk modulus for ScSe is 93.96 (93.85) GPa for the  $B1$  phase and 90.48

(90.35) GPa for the  $B2$  phase. It is clear from Table 3 that our present calculated values of bulk properties from MIPM model calculation and first principle calculations are in good agreement with available theoretical results [13] and experimental results [27].

**3.3. Electronic properties.** To study the stability of the present compound, the total electronic density of state (DOS) for both  $B1$  and  $B2$  phases have been demonstrated. The electronic band structure (BS) and density of states (DOS) for the present compound have been shown in Fig. 4

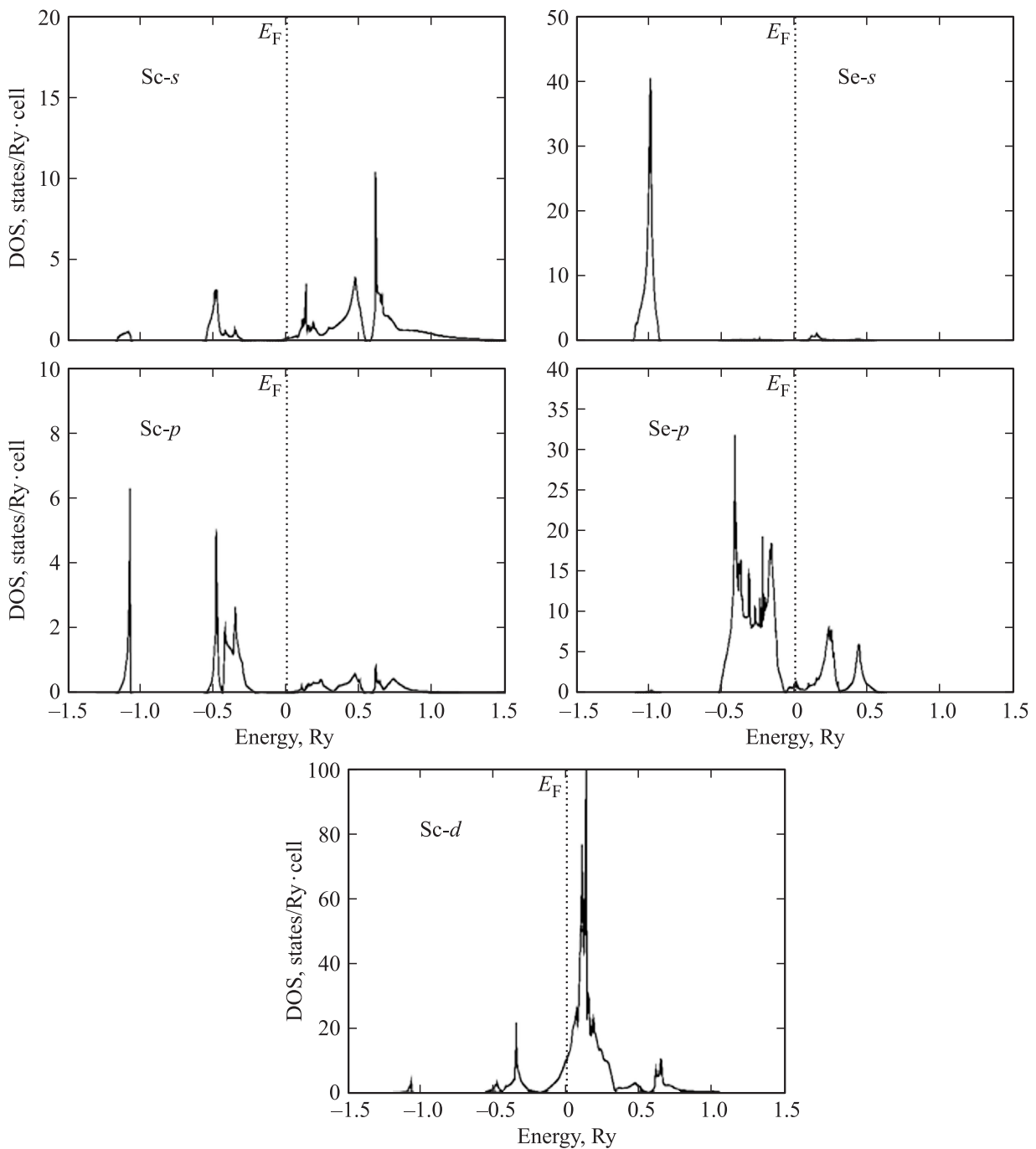


**Figure 6.** Partial density of states (PDOS) in the NaCl phase of ScSe.

in their rock-salt (*B1*) phase under ambient conditions. It is perceptibly seen from this figure that there is no energy gap near the Fermi level. This indicates a metallic nature of the present compound.

As the present compound undergoes *B1* to *B2* phase transition, to study the mechanism of the transition, we have also explored the electronic structure at high pressures in the CsCl (*B2*) phase. The electronic band structure (BS) and density of states (DOS) for the present compound are given in Fig. 5 in their CsCl (*B2*) phase. The nature of

the electronic bands of present compound with *B2* phase is the same as that of the *B1* phase. The position of different bands of the *B2* phase is shift higher in energy relative to the *B1* phase. In the CsCl (*B2*) phase more compressed bands are seen.

To understand the elementary contribution of all the atoms to the electronic structure of present compound we have studied the partial density of states (PDOS) as shown in Fig. 6. It is obvious from Fig. 6 that the lower valence band lies at -0.5Ry due to Sc-s state and -0.4Ry due to

**Table 3.** Calculated equilibrium lattice parameter  $a$  Å, bulk modulus  $B$  GPa and pressure derivative of bulk modulus ( $B'$ ) of ScSe

Properties	ScSe	
	NaCl-type	CsCl-type
Lattice parameter, Å		
(Approach I)	5.392	3.299
(Approach II)	5.389	3.296
Others	5.385 <sup>a</sup>	3.302 <sup>a</sup>
Expt.	5.398 <sup>b</sup>	–
Bulk modulus $B$ , GPa		
(Approach I)	93.96	90.48
(Approach II)	93.85	90.35
Others	95.92 <sup>a</sup>	98.466 <sup>a</sup>
Pressure derivative of bulk modulus ( $B'$ )		
(Approach I)	3.58	3.412
(Approach II)	3.53	3.867
Others	3.64 <sup>a</sup>	3.961 <sup>a</sup>

$a$  — [13],  $b$  — [25]

Sc- $d$  state. The upper valence band lies at -1.1Ry, -1.0Ry and -0.5Ry due to Sc- $p$ , Se- $s$  and Se- $p$  states respectively. Scandium- $d$  state is highly localized at the Fermi level. The conduction bands are due to the hybridization of Sc- $d$  state with a small contribution of the chalcogen- $p$  state.

#### 4. Conclusion

The electronic band structure and phase transition properties of ScSe have been studied from the model calculation (Approach I) and first principle calculations (Approach II). In the present study, initially we have predicted the ground state properties, including lattice parameter, bulk modulus and its pressure derivatives. It is found that these values from both approaches are in a good agreement with available experimental and other theoretical data for NaCl ( $B1$ ) and CsCl ( $B2$ ) structures respectively. To investigate the structural properties, we have determined the phase transformation pressure at which these compounds undergo a structural transition from  $B1$  to  $B2$  phase. The calculations for the  $B1$  to  $B2$  phase transition have been carried out in the framework both approaches. Especially for solids, LDA is computationally much simpler than HF with the true exchange potential and not as complicated as Slater's local exchange approximation. The best results from LDA are however obtained in solids, whose structural and vibrational properties are in general well described. The correct crystal structure is usually found to have the lowest energy; bond lengths, bulk moduli and phonon frequencies are accurate within a few percent. Our results on the density of states show that the present compound is a conductor with a more covalent bonding character.

#### References

- [1] T. Adachi, I. Shirotni, J. Hayashi, O. Shimomura. Phys. Lett. A **250**, 389 (1998).
- [2] J.M. Leger, I. Vedel, A.M. Redon, J. Rossat-Mignod. J. Magn. Magn. Mater. **63–64**, 49 (1987).
- [3] I. Vedel, K. Oki, A.M. Redon, J.M. Leger. Physica B + C **139–140**, 361 (1986).
- [4] C.G. Duan, R.F. Sabirianov, J. Liu, W.N. Mei, P.A. Dowben, J.R. Hardy. Phys. Rev. Lett. **94** 237201 (2005).
- [5] G. Vaitheeswaran, V. Kanchana, M. Rajgopalan. Physica B **315** (2002) 64; Alloys. Comp. **336**, 46 (2002).
- [6] Chun-Gang Duan, R.F. Sabirianov, W.N. Mei, P.A. Dowben, S.S. Jaswal, E.Y. Tsymbal. J. Phys. Condens. Matter **19**, 315220 (2007).
- [7] T. Adachi, I. Shirotni, J. Hayashi, O. Shimomura. Phys. Lett. A **250**, 389 (1998).
- [8] O. Vogt, K. Mattenberger. J. Alloys Comp. **223**, 226 (1995).
- [9] A. Tebboune, D. Rached, A. Benzair, N. Sekkal, A.H. Belbachir. Phys. Status Solidi B, **243**, 2788 (2006).
- [10] I.A. Smirnov. Phys. Stats. Solidi A **14** 363 (1972).
- [11] A.K. Singh, A. Jayaraman, A. Chatterjee. Solid State Commun. **9**, 1459 (1971).
- [12] A. Chatterjee, A.K. Singh, A. Jayaraman. Phys. Rev. B **6**, 2285 (1972).
- [13] A. Maachou, H. Aboura, B. Amrani, R. Khenata, S. Bin Omran, D Varshney. Comput. Mater. Sci. **50**, 3123 (2011).
- [14] N.E. Christensen. Phys. Rev. B **32**, 207 (1985).
- [15] O.K. Andersen. Phys. Rev. B **12**, 3060 (1975).
- [16] O.K. Andersen, O. Jepsen. Phys. Rev. Lett. **53**, 2571 (1984).
- [17] W. Kohn, L.J. Sham. Phys. Rev. A **140**, 1133 (1965).
- [18] J. Toulouse, A. Savin. J. Mol. Structure **762**, 147 (2006).
- [19] U. Van Barth, L. Hedin. J. Phys. C **5**, 1629 (1972).
- [20] V. Shrivastava, M. Rajagopalan, S.P. Sanyal. J. Magn. Magn. Mater **321**, 607 (2009).
- [21] O. Jepsen, O.K. Andersen. Solid State Commun. **9**, 1763 (1971).
- [22] F. Birch, J. Geophys. Rev. **83**, 1257 (1978).
- [23] P. Bhardwaj, S. Singh. Phys. Status Solidi B **249**, 38 (2012).
- [24] P. Bhardwaj, M. Sarwan, R. Dubey, S. Singh. J. Mol. Structure **1043**, 85 (2013).
- [25] S. Singh, P. Bhardwaj. J. Alloys Comp. **509**, 7047 (2011).
- [26] P. Bhardwaj, S. Singh. Phase Transitions A **85**, 791 (2012).
- [27] A. Svane, P. Strange, W.M. Temmerman, Z. Szotek, H. Winter, L. Petit. Phys. Status Solidi B **229**, 1459 (2001).